# Competition between C−C and C−H Activation in Reactions of Neutral Yttrium Atoms with Cyclopropane and Propene

**Ryan Z. Hinrichs, Jonathan J. Schroden, and H. Floyd Davis***

*Department of Chemistry and Chemical Biology, Cornell University, Ithaca, New York 14853*

*Received: February 22, 2003; In Final Form: August 25, 2003*

Branching ratios between C−C and C−H bond activation were measured for reactions of ground-state Y ($a^2D$, $s^2d^1$) atoms with two $C_3H_6$ isomers (cyclopropane and propene) in crossed molecular beams. For both isomers, C−C bond activation led to formation of $YCH_2 + C_2H_4$, whereas C−H activation led to $YC_3H_4 + H_2$ and $YH_2 + C_3H_4$. The angular and velocity distributions for all three product channels and for nonreactive collisions were measured at several collision energies ($E_{coll}$). For Y + cyclopropane, the branching ratio for $YCH_2 + C_2H_4$ increased relative to $YC_3H_4 + H_2$ with increasing $E_{coll}$, this C−C activation channel becoming dominant at $E_{coll} \geq 19$ kcal/mol. For the propene reaction, $\phi_{YCH_2}/\phi_{YC_3H_4}$ also increased with $E_{coll}$, reaching 0.75:1.00 at $E_{coll} = 28.8$ kcal/mol. For both $C_3H_6$ reactants, formation of $YH_2 + C_3H_4$ was observed as a minor channel at the highest collision energies. Experimental results and Rice−Ramsperger−Kassel−Marcus (RRKM) modeling indicate that for propene reactions all three channels involve initial formation of $\pi$-association complexes that undergo insertion into one of the $sp^3$-hybridized $\beta$-C−H bonds in the methyl substituent. Decay of the yttrium allyl hydride intermediate by $\beta$-H migration leads to the two C−H activation products, $YC_3H_4 + H_2$ and $YH_2 + C_3H_4$. We propose that the $YCH_2 + C_2H_4$ channel involves reverse $\beta$-H migration forming the same strongly bound metallacyclobutane intermediate formed in the Y + cyclopropane reaction.

## I. Introduction

The development of organometallic catalysts for the conversion of naturally abundant hydrocarbon feedstocks to more useful forms is a long-sought goal in organometallic chemistry. The activity of such catalysts is quite sensitive to the electronic structure of the transition metal center and to ligand and solvent effects.[1,2] Although the cleavage or "activation" of C−H bonds in solution phase inorganic chemistry is now quite well-known, the analogous process involving C−C bonds has remained elusive.[3]

To better understand how electronic structure controls transition metal reactivity, reactions of transition metal atoms and cations with hydrocarbons have been studied, both experimentally and theoretically. In reactions of transition metal cations, both C−H and C−C bond activation is quite well-known.[4−8] Calculations have demonstrated that for cation reactions, barrier heights for C−C insertion are comparable to or even lower than those for C−H insertion.[8] For example, reactions of $Fe^+$, $Co^+$, and $Ni^+$ with propane led to methane elimination via C−C insertion, as well as to molecular hydrogen elimination following C−H insertion.

The potential energy barriers for insertion of *neutral* second-row transition metal atoms into C−H and C−C bonds are considerably larger than those for cations.[9] For ethane, because the potential energy barrier heights for C−C insertion are much larger than those for C−H insertion,[9,10] no evidence for this process was observed in our previous studies.[11,12] The fundamental difference between C−H and C−C insertion for saturated hydrocarbons such as ethane has been rationalized in terms of differences in the directionality of the relevant orbitals.[13] For insertion into a C−H bond, the spherical orbital of a H atom may participate in multicenter metal−ligand bonding, leading to lower transition-state energies than those for insertion into the highly directional C−C bond.[10,13]

For cyclopropane, calculations indicate that barriers for insertion into the strained C−C bonds lie lower in energy than C−H insertion barriers for certain transition metal systems including Y and Mo.[9] Insertions into the C−H and C−C bonds are expected to be the rate-limiting steps in cyclopropane reactions with C−H insertion leading to formation of $YC_3H_4 + H_2$ and C−C insertion leading to $YCH_2 + C_2H_4$ (Figure 1).[9,14] We have recently presented a report focusing on the branching ratios between C−C and C−H activation of cyclopropane by Y, Zr, Nb, and Mo.[14] In that work, we observed a direct correlation between the product branching ratios and the calculated relative potential energy barrier heights for C−C and C−H insertion.[14]

We use the term "C−C activation" to describe any reaction leading to C−C bond fission in which the hydrocarbon is broken into two smaller hydrocarbon products with one hydrocarbon bound to the metal. It is important to note that C−C activation does not necessarily require true C−C insertion. As will be shown in this paper, the reaction of Y with propene leads to formation of $YCH_2 + C_2H_4$. The mechanism involves addition to the C═C bond followed by H atom migration and C−C bond fission, rather than by true C−C insertion.

There have been several experimental and theoretical studies of reactions of neutral transition metal atoms with propene leading to C−H activation (i.e., elimination of $H_2$). In a combined experimental and theoretical effort, Carroll and coworkers reported that both ethene and propene undergo bimolecular reaction with second-row transition metal atoms.[9] By monitoring the depletion of Y in a fast-flow reactor, Carroll et

* To whom correspondence should be addressed. E-mail: hfd1@cornell.edu.

10.1021/jp034455x CCC: $25.00 
Published on Web 10/15/2003

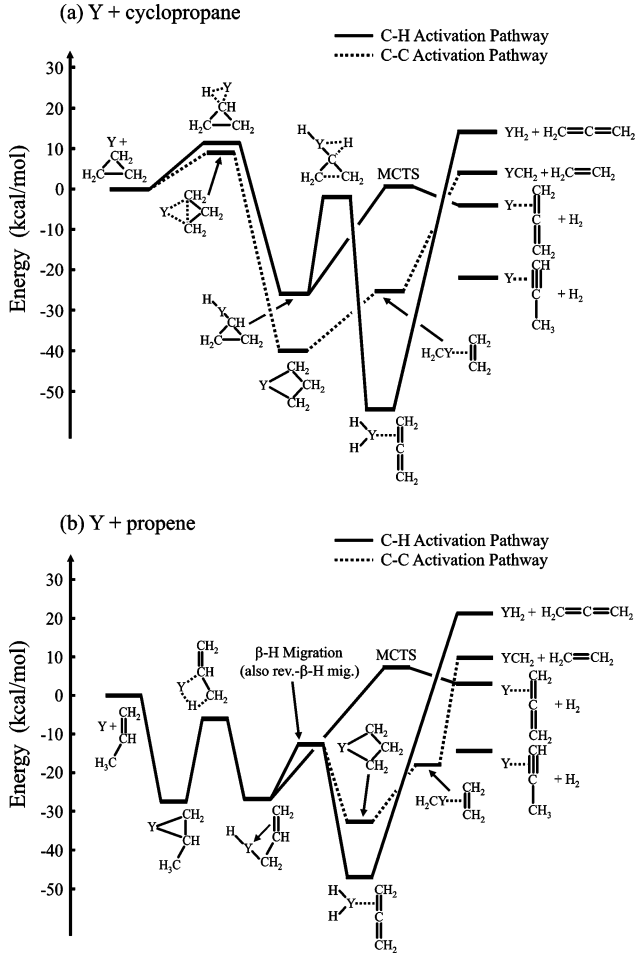


**Figure 1.** Schematic potential energy diagrams for the reactions (a) Y + cyclopropane and (b) Y + propene.[9]

al. observed effective bimolecular rate constants at 298 K of $k_1 = 8.2 \times 10^{-12}$ and $143 \times 10^{-12}$ cm$^3$ s$^{-1}$ for ethene and propene, respectively.[9] The origin of the very large difference in reactivity of the two molecules was not determined. Subsequently, Porembski and Weisshaar studied the reactions in a flow cell and directly observed $H_2$ elimination in room-temperature experiments, demonstrating that $H_2$ elimination occurs in Y atom reactions with ethene and propene even at a mean collision energy of 0.9 kcal/mol.[15] There were considerable similarities between the reaction mechanisms for Y and Zr atoms.[16] For both Y and Zr, the presence of deuterium isotope effects in ethene reactions demonstrated that the mechanism involved initial formation of $\pi$-complexes, which subsequently underwent C−H insertion forming $HMC_2H_3$. The lowest pathway to $H_2$ elimination involved concerted molecular elimination over a multicenter transition state, rather than a stepwise mechanism involving $H_2MC_2H_2$.[15,16] More recently, Bayse has shown that such multicenter transition states are also important in $H_2$ elimination in Y + $H_2CO$ reactions.[17]

In this paper, we present a study of the reactions of Y with cyclopropane and propene. Rather surprisingly, we have found that C−C activation, leading to formation of $YCH_2 + C_2H_4$, is significant even for propene reactions, particularly at higher collision energies. We have also observed some similarity between Y reactions with propene and cyclopropane. In both cases, competition between C−C activation forming $YCH_2 + C_2H_4$ and C−H activation forming $YC_3H_4 + H_2$ was observed. At the highest collision energies, an additional C−H activation channel producing $YH_2 + C_3H_4$ was also observed.

In the accompanying paper, we present results of experimental studies of reactions of Y with four butene isomers.[18] These studies confirm some of the mechanistic details inferred here and provide additional mechanistic insight. In particular, we propose that the large yield of $YCH_2 + C_2H_4$ from Y + propene results from the unfavorable nature of $\beta$-H migration necessary for the competing reaction pathways leading to C−H activation ($YC_3H_4 + H_2$ and $YH_2 + C_3H_4$). In reactions involving butenes, on the other hand, $\beta$-H migration is favorable, causing a dramatic shift in branching ratios, C−H activation being dominant and C−C activation being a minor channel.

## II. Experimental Section

The reactions were studied using a rotatable source crossed molecular beams apparatus.[19] The Y beam was produced by laser ablation from a 0.25-in. diameter rod (99% purity, Alfa Aesar) using the 532 nm output of a Nd:YAG laser (Continuum Surelite, 15mJ). A piezo-electrically actuated pulsed valve delivered an inert carrier gas that entrained the Y atoms into a supersonic expansion. The metal beam was collimated by a skimmer and a defining aperture and was temporally refined by a slotted chopper wheel before entering the main collision chamber held at or below $10^{-6}$ Torr.[19] The electronic state populations of the Y beam were previously characterized using laser-induced fluorescence spectroscopy, confirming the presence of only the two spin−orbit levels of the ground $a^2D_J$ ($s^2d^1$) electronic state.[11]

A molecular beam was generated by expanding a dilute (10−20%) mixture of $C_3H_6$ in an inert carrier gas. The beam was collimated by a skimmer before intersecting the Y beam at 90°. Neutral products were detected 24.1 cm away by photoionization using 157 nm $F_2$ excimer radiation (Lambda Physik LPX 220i) followed by mass selection and ion detection. The time-of-flight (TOF) spectra of the products were obtained by scanning the trigger of the excimer laser with respect to time zero for reaction, as defined by the chopper wheel. By rotating the two molecular beams with respect to the fixed detector, TOF spectra were recorded at various laboratory angles. Product lab angular distributions were obtained by integrating TOF spectra for each channel at 2° increments.

The product scattering distribution, $I(E,\theta)$, was assumed to be separable into the center-of-mass (CM) product translational energy, $P(E)$, and angular, $T(\theta)$, distributions. For reactions involving intermediate complexes with lifetimes far in excess of their rotational periods, as in the reactions reported here, this is a reasonable assumption. These distributions were used with the known experimental parameters (flight distances, aperture sizes, etc.) to simulate the raw TOF and angular distribution data using the forward convolution technique.[20] The CM distributions were iteratively adjusted until agreement between simulations and experimental data was obtained.

## III. Results and Analysis

**A. Yttrium + Cyclopropane: $E_{coll}$ = 18.5 kcal/mol.** For both $C_3H_6$ reactant isomers, several competing product channels were observed:

$$Y\ (a^2D_J;\ 5s^24d^1) + C_3H_6 \rightarrow YCH_2 + C_2H_4 \quad (1)$$

$$\rightarrow YC_3H_4 + H_2 \quad (2)$$

$$\rightarrow YH_2 + C_3H_4 \quad (3)$$

$$\rightarrow Y + C_3H_6 \quad (4)$$

**TABLE 1: Experimental Conditions for Y-Atom Beam**

Y + Cyclopropane

| $E_{coll}$[a] | carrier gas | velocity[b] | fwhm[b] |
|---|---|---|---|
| 11.6 | pure Ne | 1410 | 150 |
| 18.5 | 50% Ne/50% He | 1690 | 190 |
| 29.5 | pure He | 2480 | 310 |
| 36.8 | 50% He/50% $H_2$ | 2930 | 420 |

Y + Propene

| $E_{coll}$[a] | carrier gas | velocity[b] | fwhm[b] |
|---|---|---|---|
| 12.3 | pure Ne | 1380 | 130 |
| 15.8 | 50% Ne/50% He | 1680 | 190 |
| 25.2 | pure He | 2430 | 310 |
| 28.8 | 50% He/50% $H_2$ | 2570 | 350 |
| 43.2 | pure $H_2$ | 3290 | 470 |

[a] Values in kcal/mol. [b] Values in m/s.

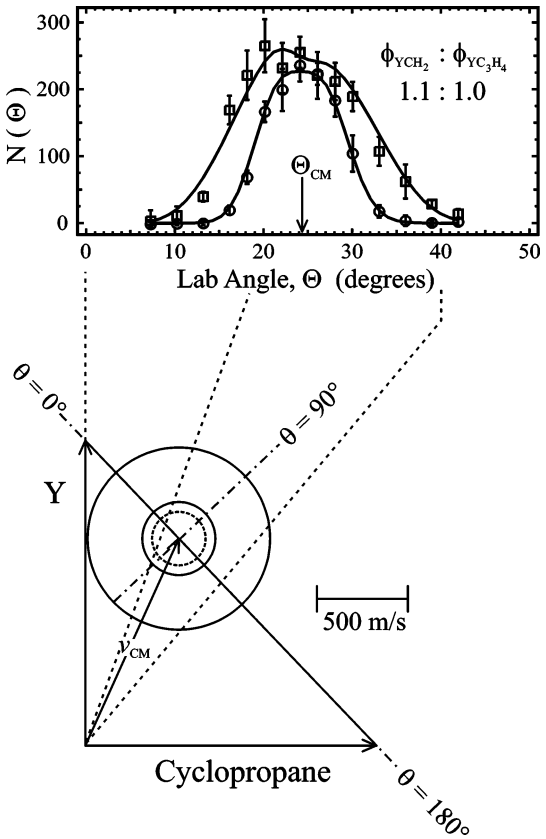


**Figure 2.** Newton diagram in velocity space for Y + cyclopropane at $E_{coll}$ = 18.5 kcal/mol. Larger solid circle corresponds to maximum velocities for $YCH_2$ products, while smaller solid circle and smaller dotted circle correspond to maximum velocities for Y−propyne and Y−allene products, respectively. Lab angular distributions for $YCH_2$ (□) and $YC_3H_4$ (○) were recorded under identical collision conditions. Solid-line fits to lab angular distributions were generated using CM distributions in Figure 4.

Collisions of Y with cyclopropane were studied at $E_{coll}$ = 9.4−36.8 kcal/mol (Table 1). The competition between $YCH_2$ + $C_2H_4$ and $YC_3H_4$ + $H_2$ was monitored at various laboratory angles by alternating scans at *m*/*e* 103 ($YCH_2^+$) and 129 ($YC_3H_4^+$). A Newton diagram in velocity space (Figure 2) depicts the relationship between the lab and CM reference frames for $E_{coll}$ = 18.5 kcal/mol. Reaction products scatter radially from the tip of the CM velocity vector, $v_{CM}$, with a maximum allowed velocity (shown as circles) determined by reaction energetics and conservation of linear momentum. As anticipated from energy and momentum conservation, the $YCH_2$ products were scattered over a wider lab angular range than the $YC_3H_4$ products because of the heavier recoiling counter-fragment ($C_2H_4$ vs. $H_2$, respectively). The *m*/*e* 103 data has been corrected for a small contribution from fragmentation of $YC_3H_4$. Representative TOF spectra are shown at indicated lab angles in Figure 3.

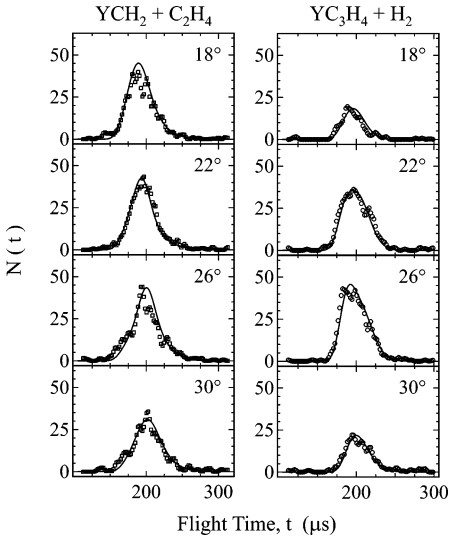


**Figure 3.** Sample TOF spectra recorded at indicated lab angles for $YCH_2$ (left) and $YC_3H_4$ (right) products from collisions of Y + cyclopropane at $E_{coll}$ = 18.5 kcal/mol (open points). Solid-line fits were generated using CM distributions in Figure 4.

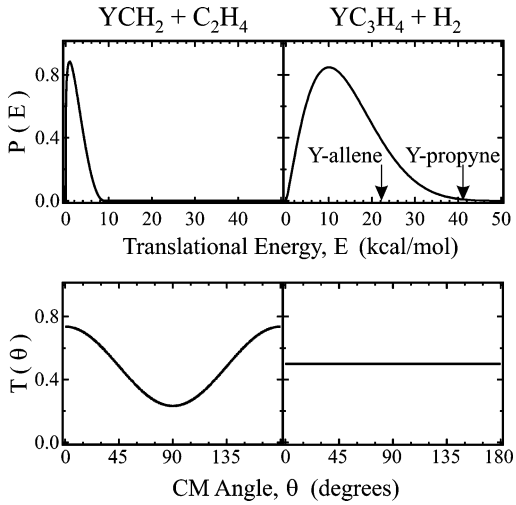


**Figure 4.** CM translational energy distributions, $P(E)$, and angular distributions, $T(\theta)$, used to simulate data from collisions of Y + cyclopropane at $E_{coll}$ = 18.5 kcal/mol. Arrows indicate maximum allowed translational energy for formation of two distinct product isomers.

The solid-line simulations included in Figures 2 and 3 were generated using the CM translational energy, $P(E)$, and angular, $T(\theta)$, distributions shown in Figure 4. The maximum allowed translational energy for formation of the two possible $YC_3H_4$ isomers, Y−allene and Y−propyne, are denoted by arrows on the energy axis of the $P(E)$. With the use of the calculated energetics for Y−propyne formation[9] along with $E_{coll}$ and $\langle P(E) \rangle$ = 14.0 kcal/mol, the average fraction of available energy deposited as translational energy ($f_T$) was 0.34. Reductive elimination of ethene was best fit with a $P(E)$ peaking closer to zero translational energy (Figure 4), such that the fraction of energy appearing in translation was $f_T$ = 0.18. For both product

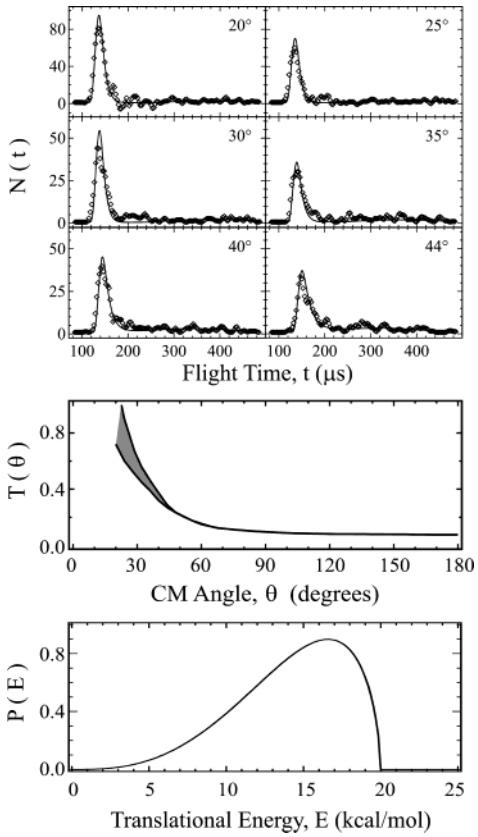


**Figure 5.** Sample TOF spectra (top) recorded at indicated lab angles for nonreactive scattering of Y atoms from collisions with cyclopropane at $E_{coll} = 18.5$ kcal/mol (open points) and CM distributions (bottom) used to generate solid-line simulations to the TOF data. Shaded area in the $T(\theta)$ indicates range of distributions that give acceptable fits to the data.

channels, the best-fit CM angular distributions are symmetric about $\theta = 90°$.[21,22]

The ratios of reaction cross sections for competing product channels may be derived from the relative signal levels if the relative ionization cross sections for the products are known. Because the 157 nm photoionization cross sections for $YCH_2$, Y−propyne, and Y−allene are not known, experiments were performed using electron impact ionization, which may be calibrated, as discussed in section III.D. These studies indicated that the ratio of $YCH_2$ to $YC_3H_4$ 157 nm photoionization cross sections is approximately unity. Determination of the branching ratio also requires explicit consideration of fragmentation during ionization. We recorded TOF spectra at all *m*/*e* values at which signal was observed and scaled the parent ion ratio accordingly. The fraction of the total product signal sampled within the detector solid angle depends on the radius of the scattering sphere in the CM reference frame. The appropriate Jacobian transformations to account for this dependence on the scattering radius are included in the forward convolution calculations used to simulate the experimental data. By scaling the normalized simulations to the experimental data, the product branching ratio at $E_{coll} = 18.5$ kcal/mol, $\phi_{YCH_2}/\phi_{YC_3H_4}$, was determined to be 1.09:1.00.

The data for nonreactively scattered Y atoms recorded at *m*/*e* 89 (Figure 5) exhibit typical features for impulsive inelastic scattering without appreciable long-lived complex formation.[11,12] At all lab angles, the fast scattering peak (∼150 $\mu$s) dominates. In the CM reference frame, the recoiling Y atoms were forward scattered as seen in the $T(\theta)$. The TOF spectra recorded approaching $\Theta = 0°$ became increasingly unreliable because

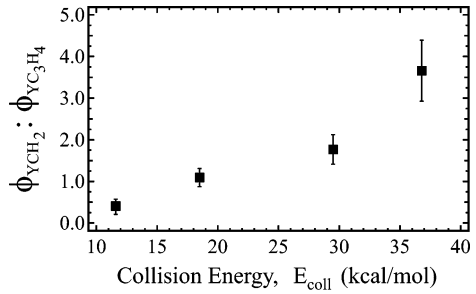


**Figure 6.** Product branching ratio, $\phi_{YCH_2}/\phi_{YC_3H_4}$, for reactions of Y + cyclopropane as a function of $E_{coll}$.

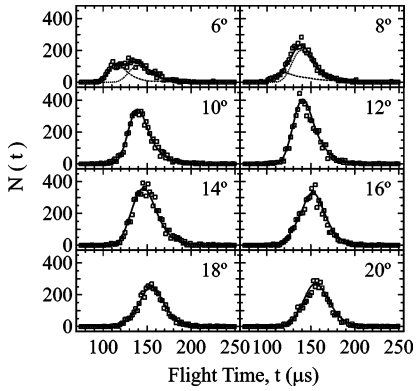


**Figure 7.** Sample TOF spectra recorded at indicated lab angles for $YCH_2$ products from collisions of Y + propene at $E_{coll} = 25.2$ kcal/mol (open points). Solid-line simulations were generated from CM distributions shown in Figure 8. Dashed line indicates overflow contribution from YO contamination in the Y atomic beam.

of contributions from the atomic beam. Consequently, the uncertainty in the $T(\theta)$ increases for CM angles $\theta < 50°$, as demonstrated by the gray shaded area included in Figure 5. By comparing $\langle P(E) \rangle$ to $E_{coll}$, it was found that ∼31% of the initial kinetic energy was converted into cyclopropane internal energy.

**B. Yttrium + Cyclopropane: Dependence on $E_{coll}$.** The product branching ratios were measured as a function of $E_{coll}$ (Figure 6). It was found that for $E_{coll} \geq 19$ kcal/mol, formation of $YCH_2$ became dominant. The CM distributions for these two product channels were found to be qualitatively similar at all $E_{coll}$ studied. Product at *m*/*e* 129 ($YC_3H_4^+$) was observed at $E_{coll}$ as low as 9.4 kcal/mol. At this $E_{coll}$, production of $YCH_2$ could not be confirmed because of background signal from YO mass overflow. At $E_{coll} = 36$ kcal/mol, a third minor product channel, $YH_2 + C_3H_4$ (recorded at *m*/*e* 91) was observed with a signal level 25 times smaller than that for $YC_3H_4$. With the use of the best-fit $P(E)$ with the energetics for $YH_2$ + allene formation, $f_T$ was 0.15.

**C. Yttrium + Propene: $E_{coll} = 25.2$ kcal/mol.** Formation of $YCH_2$ and $YC_3H_4$ was observed for the propene reaction. The experimental data recorded at *m*/*e* 129 at $E_{coll} = 25.2$ kcal/mol were similar to that observed for Y + cyclopropane at $E_{coll} = 18.5$ kcal/mol, and are therefore not shown. By considering the difference in enthalpies of formation for propene and cyclopropane, we find that these two data sets correspond to nearly the same total energy above the product asymptotes.[9] The TOF spectra at *m*/e 103, corresponding to $YCH_2^+$ (Figure 7) were recorded with a similar amount of averaging as those shown in Figure 3 and have been corrected to account for a minor contribution from fragmentation of $YC_3H_4$ as discussed below.

The solid-line fits shown in Figure 7 were generated using the CM distributions shown in Figure 8. For $YCH_2$, $\langle P(E) \rangle =$

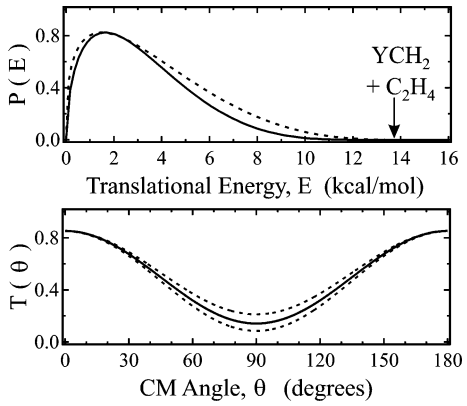


**Figure 8.** CM distributions for $YCH_2 + C_2H_4$ from collisions of Y + propene at $E_{coll} = 25.2$ kcal/mol. Arrow in the $P(E)$ indicates maximum allowed translational energy. Dashed lines correspond to range of distributions that give acceptable fits to the data.

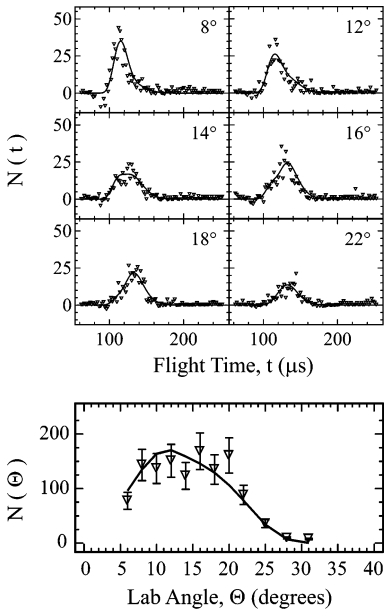


**Figure 9.** Sample TOF spectra (top) recorded at indicated lab angles for $YH_2$ products from collisions of Y + propene at $E_{coll} = 28.8$ kcal/mol (open points) and lab angular distribution (bottom) generated by integrating TOF spectra.

3.18 kcal/mol, giving $f_T = 0.23$. The $T(\theta)$, however, was identical to that shown in Figure 4 for the cyclopropane reaction. At small lab angles ($\Theta \leq 8°$), an additional fast component (i.e., short flight times) appears in the TOF spectra due to YO overflow signal. Dashed lines shown in the TOFs at 6° and 8° were obtained by fitting data recorded at *m*/*e* 105 (the source of the overflow) and have been scaled accordingly. The product branching ratio, $\phi_{YCH_2}/\phi_{YC_3H_4}$, at $E_{coll} = 25.2$ kcal/mol was 0.48:1.00.

The minor $YH_2 + C_3H_4$ channel was observed for the propene reaction at $E_{coll} = 28.8$ kcal/mol, as shown in Figure 9. For $YH_2$, $\langle P(E) \rangle = 3.7$ kcal/mol, which yields $f_T = 0.32$. The $T(\theta)$ was strongly polarized with $T(0°)/T(90°) = 12^{+6}_{-4}$. The $YH_2$ channel was 45 times weaker than for $YC_3H_4$ at $E_{coll} = 28.8$ kcal/mol.

The TOF spectra recorded at *m*/*e* 89 (Figure 10), corresponding to nonreactive Y + propene collisions, are distinctly different from corresponding data obtained for cyclopropane. At wider lab angles, the slower peak (~175 $\mu$s) becomes more intense than the fast peak. This behavior is very similar to that seen previously in our studies of reactions of transition metal atoms

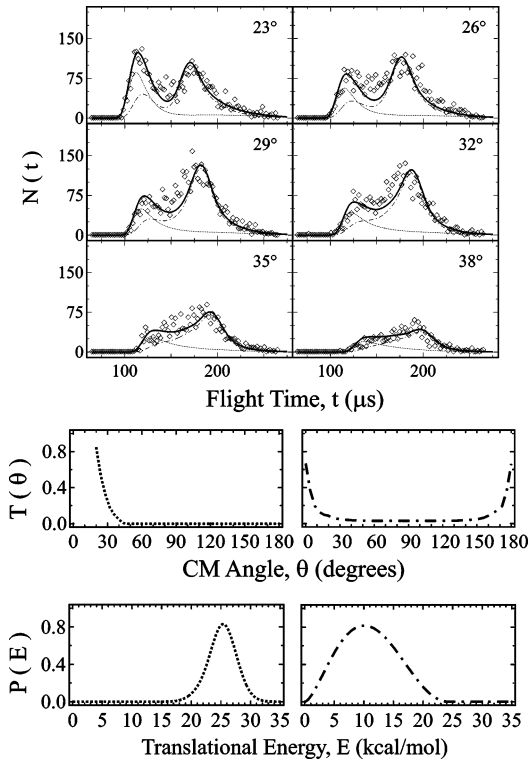


**Figure 10.** Sample TOF spectra (top) recorded at indicated lab angles for nonreactive scattering of Y atoms from collisions with propene at $E_{coll} = 28.8$ kcal/mol (open points) and CM distributions (bottom) used to generate simulations to the TOF data. Solid-line fits are the sum of the dashed and dash−dot lines. See text for details.

with $C_2H_4$,[23] $C_2H_2$,[24] and carbonyl-containing species such as $H_2CO$,[25] and clearly results from decay of $\pi$-complexes back to reactants. As in the previous studies, data was simulated using two separate $P(E)$ and $T(\theta)$ combinations (Figure 10). In one combination (shown on the right), $T(\theta)$ was constrained to forward−backward symmetry, corresponding to long-lived complexes that survive many rotational periods prior to decay back to reactants.[23,24] A second forward-scattered $T(\theta)$ corresponds to direct nonreactive collision events that do not persist for time scales longer than their rotational periods.

**D. Yttrium + Propene: Dependence on Collision Energy.** At $E_{coll} = 12.3$ kcal/mol, formation of $YC_3H_4 + H_2$ was observed (Figure 11). Weak signal was also observed at *m*/*e* 103, the mass corresponding to $YCH_2^+$, but comparison of the data recorded at *m*/*e* 103−129 at this $E_{coll}$ revealed that the weak *m*/*e* 103 signal originates primarily from fragmentation of $YC_3H_4$ during photoionization. The intensity of fragmentation signal at *m*/*e* 103 was 3.6% of the parent ion signal (*m*/*e* 129). The same value was obtained at $E_{coll} = 10.4$ kcal/mol and was used to correct the $YCH_2$ data at all $E_{coll}$. The best-fit $P(E)$ (Figure 11 bottom) indicated that $f_T = 0.46$. The product flux distributions for the two major product channels, $YC_3H_4$ and $YCH_2$, are shown in Figure 12.

For reaction with propene, $YCH_2$ product was clearly observed at $E_{coll} \geq 15.8$ kcal/mol. The complete set of lab angular distributions recorded for reactions of Y + propene at different collision energies is shown in Figure 13. Although an increase in the relative amount of $YCH_2$ formed was observed as $E_{coll}$ increased, $YC_3H_4$ formation was always dominant. The reaction with propene was also studied using electron impact ionization at $E_{coll} = 31.2$ kcal/mol. Because much longer averaging was required for each TOF, data were only recorded at the CM laboratory angle ($\Theta_{CM} = 14°$) and one angle outside

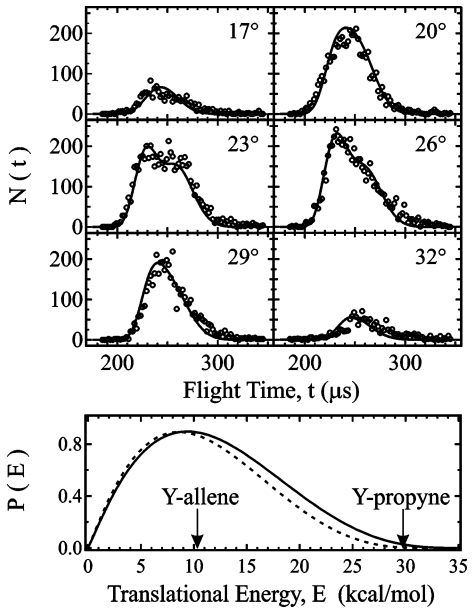


**Figure 11.** Sample TOF spectra (top) recorded at indicated lab angles for $YC_3H_4$ products from collisions of Y + propene at $E_{coll}$ = 12.3 kcal/mol (open points) and $P(E)$ (bottom) used to generate solid-line fits. Arrows indicate maximum translational energy for two distinct $YC_3H_4$ product isomers. Dashed lines correspond to range of distributions that give acceptable fits to the data.

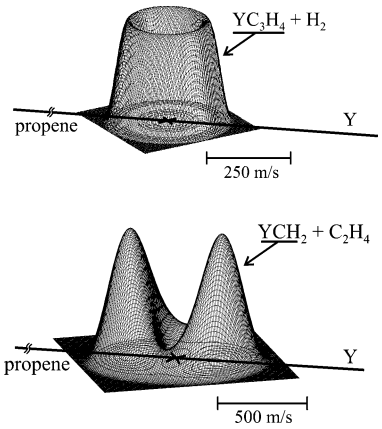


**Figure 12.** $YC_3H_4$ and $YCH_2$ product flux distributions from collisions of Y + propene at $E_{coll}$ = 12.3 and 25.2 kcal/mol, respectively. Arrows represent the CM relative velocity vectors for the colliding reactants.

the range of $YC_3H_4$ scattering ($\Theta = 20°$). Figure 14 shows the data recorded for the $YCH_2$ and $YC_3H_4$ parent ion signals. The solid-line fits were generated using CM distributions obtained from analysis of data obtained at the same $E_{coll}$ recorded using 157 nm photoionization. To fit the *m*/*e* 103 data, it was evident that fragmentation from $YC_3H_4$ must be considered. The dotted-line fit at 14° represents this fragmentation, while the dashed line indicates the $YCH_2$ signal from ethene elimination. The raw branching ratio, $\phi_{YCH_2}/\phi_{YC_3H_4}$, was 0.80:1.00. Using electron impact ionization, we relate the ionization cross section, $\sigma_{ion}$ (Å$^3$), to the molecular polarizability, $\alpha$ (in Å$^2$), using the empirical formula[26]

$$\sigma_{ion} = 36\sqrt{\alpha} - 18 \qquad (5)$$

The molecular polarizabilities for $YC_3H_4$ and $YCH_2$ were calculated by adding the Y atomic polarizability to the propyne and carbene polarizabilities. Using eq 5, we found $\sigma_{ion}$ to be 163 and 176 Å$^2$ for $YCH_2$ and $YC_3H_4$, respectively. The

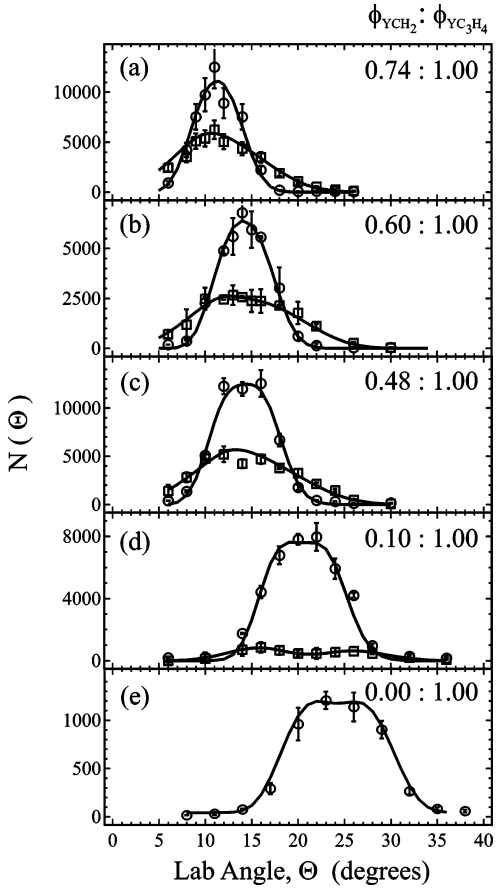


**Figure 13.** Lab angular distributions for $YC_3H_4$ (○) and $YCH_2$ (□) from collisions of Y + propene at $E_{coll}$ = (a) 43.2, (b) 28.8, (c) 25.2, (d) 15.8, and (e) 12.3 kcal/mol. Product branching ratio, $\phi_{YCH_2}/\phi_{YC_3H_4}$, is included in top right corner.

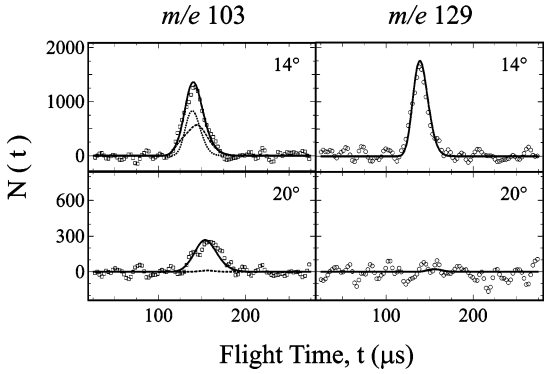


**Figure 14.** Sample TOF spectra recorded at indicated lab angles and *m*/*e* setting using electron impact ionization at $E_{coll}$ = 31 kcal/mol. Signal at *m*/*e* 103 includes contribution from $YCH_2$ (dashed line) and fragmentation of $YC_3H_4$ (dotted line).

branching ratio as corrected to include the relative ionization cross sections was $\phi_{YCH_2}/\phi_{YC_3H_4}$ = 0.74:1.00. This is shown in Figure 15 (▲), along with the values obtained using 157 nm photoionization (■). The agreement of these separate measurements shows that the ratio of 157 nm photoionization cross sections for the competing product channels is approximately unity.

## IV. Discussion

**A. Nonreactive Scattering in Cyclopropane and Propene Reactions.** For Y + cyclopropane, the forward peaking of the Y angular distribution (Figure 5) is similar to that reported

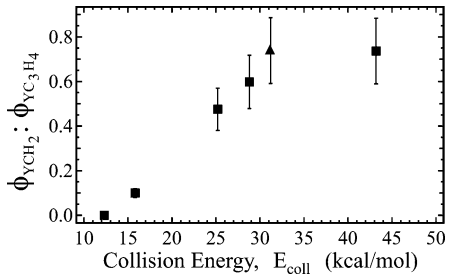


**Figure 15.** Product branching ratio, $\phi_{YCH_2}/\phi_{YC_3H_4}$, from collisions of Y + propene as a function of $E_{coll}$ obtained using 157 nm photoionization (■) and electron impact ionization (▲).

previously for saturated hydrocarbons such as ethane.[11,12] The absence of a peak at large laboratory angles indicates that there is no significant contribution from formation of long-lived intermediates decaying back to reactants. The approach of a neutral metal atom toward the strained C−C bond is sometimes considered analogous to metal−olefin interactions, in which the strained $\sigma$ C−C orbital (HOMO) and the $\sigma^*$ orbital (LUMO) interact with the metal atom.[27] One might, therefore, anticipate formation of a $\sigma$-complex prior to C−H or C−C insertion. Indeed, such $\sigma$-complexes involving either C−H or C−C bonds in cyclopropane have been implicated as intermediates in reactions of unsaturated transition metal complexes in solution with many alkanes and cycloalkanes. For example, Bergman and co-workers studied the reaction of $C_5(CH_3)_5RhCO$ with hydrocarbons including cyclopropane at low temperatures in solution.[28] In their experiment, the photolytically generated unsaturated $C_5(CH_3)_5RhCO$ complex was found to insert spontaneously into the C−H bond of cyclopropane. When the sample was warmed, the kinetically favored C−H insertion complex was found to undergo rearrangement to the more thermodynamically favorable C−C inserted metallacyclobutane complex. Detailed kinetic studies revealed that the mechanism involves reductive elimination from the C−H complex, forming the weakly bound $\sigma$-complex, which then underwent C−C insertion.[28] The absence of initial direct C−C insertion was attributed to steric effects imposed by the bulky ligands on the metal complex.

For bare transition metal atom reactions with hydrocarbons such as cyclopropane, the small local minimum corresponding to $\sigma$-bound complexes should be no deeper than several kilocalories per mole. At the relatively high collision energies of our experiment, the small $\sigma$-binding energies, comparable to those in van der Waals species, cannot support $\sigma$-bound complexes for time scales greater than their rotational periods. Therefore, for Y + cyclopropane, C−C and C−H bond insertion are direct processes without initial $\sigma$-complex formation. Insertion into cyclopropane C−H and C−C bonds has been reported previously in reactions of transition metal complexes in solution,[3] cation reactions in gas-phase guided beam experiments,[29,30] and neutral transition metal atoms in low-temperature matrixes.[31]

The reaction dynamics are quite different for Y + propene. The wide angle nonreactive scattering (Figure 10) with a slow feature appearing in the TOF spectrum near 180 $\mu$s is very similar to that seen previously in reactions of alkenes and alkynes.[23,24] This behavior indicates that a substantial fraction of initially formed complexes decay back to reactants rather than forming chemical products. The approach of neutral metal atoms to alkenes is commonly described by the Dewar−Chatt−Duncanson model,[32] in which addition of an alkene double bond to the metal atom involves both donation from the $\pi$-bonding orbital (HOMO) to an empty metal s orbital (LUMO) and back-donation from a metal d orbital (HOMO) into the $\pi^*$-antibonding orbital (LUMO). Depending on the extent of back-donation, this results in either a "$\pi$-complex," in which the double bond remains intact, or a "metallacyclopropane" complex, so-called because the double bond is broken and two covalent bonds are formed between the metal and the two carbon atoms in a three-member ring.[33,34] Recent calculations on the reaction of Y + $C_2H_4$ have found no barrier to formation of a $YC_2H_4$ $\pi$-complex,[15] which is expected to readily convert to a more stable doublet metallacyclopropane[9,15] complex, which may go on to form products or decay back to reactants.[23,24]

**B. $YC_3H_4$ + $H_2$ from the Cyclopropane Reaction.** For Y + cyclopropane, $H_2$ elimination was significant at all collision energies studied. Several stationary points along the reaction pathway have been calculated.[9] From the ground-state reactants, a doublet C−H insertion transition state lying at +11.3 kcal/mol leads to a $HYC_3H_5$ insertion intermediate lying 26.9 kcal/mol below the separated reactants (Figure 1).[9] We observed $H_2$ elimination at collision energies as low as 9.4 kcal/mol. Because spin−orbit excited Y ($a^2D_{5/2}$) atoms, which contribute 1.5 kcal/mol of electronic energy, are known to be present in our beam,[24] our observations indicate that the calculated C−H insertion barrier of 11.3 kcal/mol is a strict upper limit.

The observation of significant translational energy in the $YC_3H_4$ + $H_2$ products ($f_T$ = 0.34) suggests the presence of a potential energy barrier along the exit channel reaction coordinate. Similar behavior has been observed in our laboratory for reactions of Y with acetylene,[24] ethene,[23] ethane,[12] and formaldehyde[25] and is explained by the existence of a multicentered transition state (MCTS) just prior to $H_2$ elimination, lying slightly higher in energy than the product asymptote.[15−17]

By analogy with all Y reactions studied previously in our laboratory, $H_2$ elimination is initiated by insertion into one of the C−H bonds in cyclopropane, forming $HMC_3H_5$. In the room-temperature flow cell experiments, the reaction rate constant for Y + cyclopropane was very small, $0.7 \times 10^{-12}$ $cm^3s^{-1}$.[9] It was suggested that the reaction most likely involved termolecular stabilization of C−H or C−C insertion complexes rather than molecular elimination.[9] Although no calculations on this process have been carried out, the dynamically most favorable route to $H_2$ loss in this case is likely via α-H atom migration (migration of the single H atom remaining on the metal-bound carbon atom) to the Y−H moiety with concerted $H_2$ elimination over a multicenter transition state.[15−17] This process involves ring opening with formation of allene with no H atom migration necessary. Elimination of propyne, which is thermodynamically more favorable than loss of allene,[9] requires H atom rearrangement. From the maximum translational energy distribution shown in Figure 11, at least 30% of the $C_3H_4$ products are indeed propyne, indicating the occurrence of H atom migration during $H_2$ loss. In light of the large amount of available energy, H atom migration is not at all surprising.

**C. $YCH_2$ + $C_2H_4$ from the Cyclopropane Reaction.** Insertion into the C−C bond of cyclopropane results in formation of the metallacyclobutane intermediate, lying 40.0 kcal/mol below the reactants.[9] This complex, which involves a four-membered ring containing the metal and three carbon atoms, can decay to form $YCH_2$ + $C_2H_4$ by simple electronic rearrangement with simultaneous fission of one C−C bond and one Y−C bond. No isomerization or H atom migration is necessary. Therefore, direct ethene elimination from the metallacyclobutane is expected to be dynamically favorable. Indeed, there is extensive precedence in the organometallic chemistry literature for this process in both the forward and reverse direction.[35,36] In particular, an important key step in the olefin

metathesis reaction involves the addition of ethene to a metal carbene, forming a metallacyclobutane, that is, the exact reverse of the mechanism proposed here.[35,36] In Figure 1, a possible intermediate along the reaction pathway, $CH_2YC_2H_4$, is included. To assess the possibility that this species can be accessed, consider the reverse reaction, addition of a metal carbene to ethene. The electronic configuration of $YCH_2$ ($5s^14d^2$)[37] can readily add to the ethene double bond to form a $CH_2YC_2H_4$ complex through a barrierless transition state. This complex is strongly bound with respect to ethylene loss, suggesting that it represents a true local minimum on the reaction coordinate.[9] The small translational energy release ($f_T = 0.18$) observed for ethylene loss and the large yield of $YCH_2$ is consistent with a loose transition state for loss of ethylene from the metallacyclobutane.

Formation of $YCH_2 + C_2H_4$ is thermodynamically less favorable than production of $YC_3H_4 + H_2$. However, 1,1-$H_2$ elimination from the $sp^3$-hybridized carbon atoms in the metallacyclobutane complex will likely encounter large potential energy barriers. Therefore, $H_2$ elimination would require H atom migration or reductive elimination by passage back over the high C−C insertion barrier. For transition metal atom reactions under collision-free conditions, reductive elimination would lead to reformation of reactants with essentially no probability of getting trapped in the shallow $\sigma$-complex well. These considerations, in addition to a large body of inorganic literature,[3,27] indicate that $C_2H_4$ rather than $H_2$ elimination is the dominant decay pathway following C−C insertion. This leads us to believe that the metallacyclobutane complex decays exclusively to $YCH_2 + C_2H_4$. Similarly, C−H insertion in cyclopropane leads to efficient $H_2$ elimination. Because the rate-limiting steps for both C−C and C−H activation reactions are the initial insertion processes and because interconversion between C−C and C−H insertion complexes is not likely to compete with molecular elimination forming products, we conclude that the branching ratio between $YCH_2$ and $YC_3H_4$ in the cyclopropane experiments is the branching ratio for initial C−C to C−H insertion. This is supported by our previous experiments in which the $MCH_2/MC_2H_4$ branching ratios for Y, Nb, Zr, and Mo reactions with cyclopropane were correlated to the relative barrier heights for C−C and C−H insertion rather than to the thermodynamics of product formation.[14]

**D. $YC_3H_4 + H_2$ and $YH_2 + C_3H_4$ from the Propene Reaction.** Our finding that the reaction Y + propene → $YC_3H_4 + H_2$ was observed at all collision energies is certainly not surprising in light of the fact that Porembski and Weisshaar observed $H_2$ elimination at a mean collision energy of only 0.9 kcal/mol.[15] We observe $YC_3H_4$ signal from the propene reaction to be 15 times more intense than that from cyclopropane at $E_{coll} = 12$ kcal/mol. Clearly the reactivity of propene results from the large capture cross section for formation of $\pi$-complexes, a process that has been shown theoretically to proceed for Y + ethene with no significant potential energy barrier.[15] This contrasts the situation for reactions of alkanes including cyclopropane that must be initiated by direct insertion over relatively tight transition states.[9]

As already noted, it has been known for some time that the reaction rate constant is much larger for propene than for ethene at room temperature.[9] To date, however, no definitive explanation for this behavior has been offered. It has been pointed out that the larger density of states for the metal $\pi$-complex resulting from the presence of a methyl group in propene will lead to increased complex lifetimes relative to those for ethene.[9,15] This increased lifetime could increase the probability of termolecular stabilization in the flow-cell experiments. However, in those experiments, it was concluded that the Y + ethene and propene reactions were bimolecular,[9] not termolecular, and $H_2$ products have been observed.[15] In the absence of collisional stabilization, the branching ratio for decay of complexes to products relative to decay back to reactants depends on the total energy and the nature of the transition states for the competing processes, independent of well depth and lifetime of the common complex. Thus the increased density of states in propene relative to ethene cannot explain the greater rate constant for propene relative to ethene. Because steric hindrance should be greater for propene, these considerations would lead to the conclusion that propene should be less reactive, not more reactive, than ethene.

We have previously studied the reactions of several second-row transition metal atoms, including Y, with ethene.[23] To understand why propene is more reactive than ethene, we have measured the branching ratios for decay of $\pi$-complexes to products relative to that for decay back to reactants. This measurement was accomplished by including all reactive contributions with explicit inclusion of fragmentation effects upon 157 nm photoionization. The nonreactive scattering channel was evaluated by monitoring wide angle signal appearing at long flight times (Figure 10) for each reactant system.[23] We find that the ratio for propene and butene is larger than that for ethene by nearly an order of magnitude. This indicates that the potential energy barrier for the rate-limiting step in the reaction must be substantially smaller for propene and butene than for ethene. Because the potential energy barriers for insertion of the metal center into the vinylic C−H bonds in each system should not differ appreciably, we conclude that the large difference in reactivity must result from the presence of one or two methyl groups in the propene and butene reactants, respectively. The methyl groups apparently open up an important low-energy reaction pathway that was not available in the ethene reactions.

Reactions of ethene, propene, and butenes are initiated by formation of $\pi$-complexes. For ethene, reaction involves C−H insertion into one of the four relatively strong $sp^2$-hybridized C−H bonds. In the case of propene (and the butenes), although C−H insertion into an $sp^2$ C−H bond can occur, the alternative process involving insertion into the weaker $sp^3$-hybridized methyl C−H bonds is also possible. The potential energy barrier for insertion of a free ground-state Y($s^2d^1$) atom into the C−H bond of ethane is large (20 kcal/mol).[9,12] This is primarily associated with the inert gaslike $s^2$ repulsion of the ground-state atomic configuration (e.g., $s^2d^1$ for Y). However, formation of the ground-state Y−propene $\pi$-complex leads to considerable electronic rearrangement at the metal center with considerable rehybridization to $s^1d^2$ electronic character,[33] substantially decreasing the barrier height for intramolecular $\beta$-C−H insertion into the methyl C−H bonds in propene. The much greater reactivity of propene inferred from our experiments and those of Carroll[9] strongly suggests that this barrier height must be substantially smaller than that for insertion into $sp^2$-hybridized vinylic C−H bonds. The observation of a substantial deuterium isotope effect observed by Porembski and Weisshaar[15] for reactions of ethene but not those of propene also strongly suggests that the C−H insertion barrier following $\pi$-complex formation is substantially smaller for propene than for ethene.

We propose the mechanism for C−H activation of propene illustrated in Figure 16. Formation of a $\pi$-complex is followed by insertion into a methyl C−H bond, leading to formation of $HYCH_2CHCH_2$. This species may be represented by several resonance structures: Two involve a single Y−C bond with

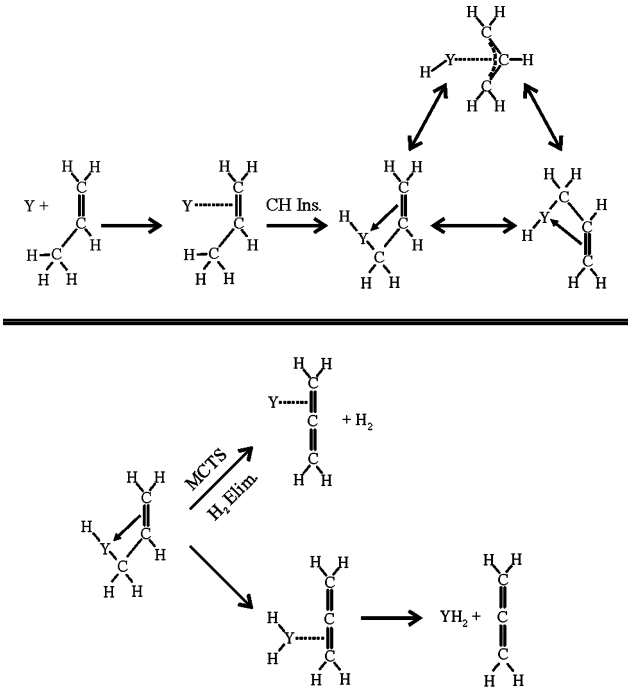


**Figure 16.** Proposed reaction mechanism (top) for Y + propene. Addition to the C═C bond leads to formation of a $\pi$-complex, followed by intramolecular insertion into a methyl C−H bond. Three resonance structures may be written for the resulting allyl hydride complex. The bottom panel shows the mechanism for C−H activation of propene. Decay of the allyl hydride complex may proceed via migration of the lone vinyl H atom ($\beta$-H migration). Migration may proceed toward the Y−H moiety via a MCTS, forming $YC_3H_4 + H_2$, or alternatively to Y forming $H_2YC_3H_4$, which subsequently decomposes by simple ligand loss to give $YH_2 + C_3H_4$.

added stabilization resulting from donation of $\pi$-electron density into the unoccupied levels of the metal, as indicated by the arrow. A third resonance contribution involves a symmetric allyl-type structure. Transfer of the single hydrogen atom from the central carbon atom, known as "$\beta$-H migration" in the inorganic literature, is well-known to be the primary decomposition pathway for transition metal alkyl complexes having $\beta$-H atoms; such complexes tend to be much less kinetically stable than those without $\beta$-H atoms.[38,39] As indicated in the bottom portion of Figure 16, this H atom may be transferred to the H atom already present on the metal, leading to $H_2$ elimination via a multicenter transition state, forming the metal−allene complex. Alternatively, $\beta$-H migration to the metal (rather than to the H atom bound to the metal) can lead to production of a Y allyl dihydride complex, which can subsequently eliminate allene. This is analogous to mechanisms believed to play important roles in formation of $YH_2$ in reactions of Y with ethane[12] and formaldehyde.[17,25]

**E. $YCH_2 + C_2H_4$ Formation from Propene Reactions.** The observation of $YCH_2$ + ethylene from the Y + propene reaction illustrates the cleavage of an unstrained C−C bond in a neutral metal−hydrocarbon reaction. We were quite surprised that the $YCH_2$ yield is nearly as large as that for $YC_3H_4$ at high collision energies, despite the much less favorable thermodynamics for this channel (Figure 1). We now consider possible mechanisms for intramolecular rearrangement of the initially formed Y−propene $\pi$-complex to $YCH_2 + C_2H_4$. One possible mechanism involves immediate insertion into the $sp^2-sp^3$ C−C bond adjacent to the oxidized C═C bond in the Y−propene complex, as shown in Figure 17. The resulting $Y(CH_3)(CH═CH_2)$ intermediate could further rearrange via α-C−H insertion to form $YCH_2(H)(CH═CH_2)$. Transfer of an H atom then gives

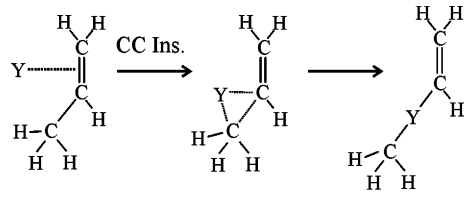


**Figure 17.** Possible mechanism for C−C activation involving formation of a $\pi$-complex followed by direct $sp^2-sp^3$ C−C insertion. This mechanism is ruled out on the basis of the much larger potential energy barrier for C−C insertion relative to C−H insertion from the $\pi$-complex.

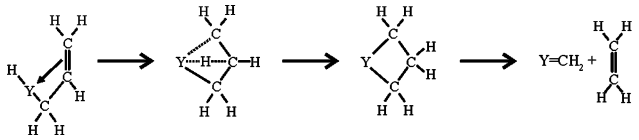


**Figure 18.** Mechanism for C−C activation of propene. Decay of the allyl hydride complex may proceed via migration of the metal-bound H atom to the $\beta$-carbon atom in the allyl moiety (i.e., reverse $\beta$-H migration), leading to formation of the same metallacyclobutane complex implicated in the Y + cyclopropane reaction. The dynamically most favorable decay pathway is to $YCH_2 + C_2H_4$.

$CH_2YC_2H_4$ which can decay to $YCH_2 + C_2H_4$ products. Again with the reasonable assumption made that all propene reactions originate from a common $\pi$-complex, the product branching ratio $\phi_{YCH_2}/\phi_{YC_3H_4}$ is the ratio of the rate for C−C insertion ($k_{CC}$) to that for C−H insertion ($k_{CH}$) from the initial $\pi$-complex. Thus Rice−Ramsperger−Kassel−Marcus (RRKM) theory may be used to calculate $k_{CC}(E)/k_{CH}(E)$. As has been described in detail,[40] we have carried out RRKM calculations and, not surprisingly, have found that the large yields of $YCH_2 + C_2H_4$ require that the largest potential energy barrier along the reaction coordinate cannot be significantly larger than that for $H_2$ elimination. Therefore, the potential energy barrier for C−C insertion cannot significantly exceed that for C−H insertion. However, theoretical calculations[9,10] and molecular orbital arguments[13] always indicate that C−C insertion barriers are significantly larger than those for C−H insertion, except in systems containing ring strain. For us to successfully model the observed branching ratios, which become nearly 1:1 at the highest collision energies, would require a C−C insertion barrier that is nearly identical to that for the C−H bond, which is not a likely possibility. Thus the $sp^2-sp^3$ C−C insertion mechanism shown in Figure 17 cannot be a primary mechanism for $YCH_2$ formation in the Y + propene reaction.

We believe that in the propene reaction the large yield of $YCH_2 + C_2H_4$ results from a mechanism very similar to that for production of $YH_2 + C_3H_4$ and $YC_3H_4 + H_2$. As already discussed, following $\pi$-complex formation, insertion of the metal center into one of the methyl C−H bonds leads to production of $HYCH_2CHCH_2$. In the previous mechanism, $\beta$-H migration to the metal or to the H atom leads to the C−H activation products $YH_2 + C_3H_4$ and $YC_3H_4 + H_2$, respectively. However, if the *metal-bound H atom* instead migrates to the $\beta$-carbon (i.e., to the central carbon in allyl), the *same* metallacyclobutane complex implicated in the cyclopropane reaction is formed through ring closure (Figure 18). As indicated in Figure 1, the metallacyclobutane complex will preferentially decay to $YCH_2 + C_2H_4$ by simple electronic rearrangement, as in the cyclopropane reaction.

The importance of C−H insertion into the methyl group of propene following $\pi$-complex formation has not been previously realized. We believe that this channel is common to all three reaction pathways. Clearly, the relative branching ratios for C−H to C−C activation depend on the competition between

$\beta$-H migration *from* the allyl complex relative to that involving motion *toward* the allyl complex. It is well-known to organometallic chemists that successful synthesis of C−H activation complexes resistant to decomposition usually requires design strategies in which the presence of $\beta$-H atoms can be avoided.[38,39] This is because decomposition is most favorable via $\beta$-H migration to the metal via energetically favorable planar transition states. For propene reactions, only a single $\beta$-H atom is present in the complex formed by insertion into one of the three $sp^3$-hybridized C−H bonds. This lone $\beta$-H atom is bonded to an $sp^2$-hybridized carbon atom (Figure 16, top), and is therefore rather strongly bound, leading to relatively low rate constants for C−H bond activation by $\beta$-H migration. Consequently, for propene reactions, the channel leading to production of $YCH_2 + C_2H_4$ can successfully compete.

As will be discussed in the following paper, the much smaller yield of $YCH_2$ from the Y + butene reactions is a direct result of the greatly increased rate constant for $\beta$-H migration in these systems, due to the presence of methyl groups yielding $\beta$-H atoms.[18] As will be shown, this leads to large yields of $YH_2$ and $YC_4H_6$ via C−H activation. Interestingly, isobutene (1,1-dimethylethene) is a notable exception, having no detectable $YH_2$ products due to the absence of $\beta$-H atoms.[18]

## V. Conclusions

Nonreactive scattering of Y from cyclopropane and propene were found to differ substantially. For cyclopropane, inelastic scattering peaked in the forward CM direction implicating a "fast" (i.e., less than one rotational period) scattering event. In contrast, a second nonreactive scattering process with strong backward scattering was observed for Y + propene, indicating a mechanism involving a long-lived complex that subsequently decayed back to reactants.

Two main product channels were observed from collisions of Y with cyclopropane and propene: $YCH_2 + C_2H_4$ and $YC_3H_4 + H_2$. A third minor product channel, $YH_2 + C_3H_4$, was detected, but only at high $E_{coll}$. For Y + cyclopropane, formation of $YCH_2$ was dominant at $E_{coll} \geq 19$ kcal/mol. This facile C−C activation is driven in part by relief of cyclopropane ring strain. Although the $YCH_2$ product lies relatively high in energy, because the branching ratio between C−C and C−H activation of cyclopropane is determined by the relative importance of C−C and C−H insertion, this high-energy pathway is in fact dominant at high collision energies. For Y + propene, on the other hand, $H_2$ elimination was dominant at all $E_{coll}$ studied. The dynamics of the propene reaction are dictated by the competition involving H atom migration following $\pi$-complex formation and C−H activation of the methyl group. Because $\beta$-H migration from the vinyl position is thermodynamically and statistically unfavorable for propene, the initial C−H insertion complex can undergo a different H atom migration process to form the same metallacyclobutane complex formed in the cyclopropane reaction. This novel mechanism for activation of an unstrained C−C bond provides a dynamically favorable route to production of the thermodynamically less-favorable $YCH_2 + C_2H_4$ products.

**Acknowledgment.** This work was supported by the National Science Foundation. R.Z.H. and J.J.S. thank the Department of Education for Graduate Fellowships. We thank Maurice Teo for assistance with some of the experiments. The authors have benefited greatly by the detailed mechanistic insight provided through numerous discussions with Professor Paul Chirik.

## References and Notes

(1) (a) Crabtree, R. H. *Chem. Rev.* **1985**, *85*, 245. (b) *Chem. Rev.* **1995**, *95*, 987.

(2) (a) Shilov, A. E.; Shul'pin, G. B. *Chem. Rev.* **1997**, *97*, 2879. (b) Hall, C.; Perutz, R. N. *Chem. Rev.* **1996**, *96*, 3125.

(3) Rybtchinski, B.; Milstein, D. *Angew. Chem., Int. Ed.* **1999**, *38*, 870.

(4) (a) van Koppen, P. A. M.; Bowers, M. T.; Fisher, E. R.; Armentrout, P. B. *J. Am. Chem. Soc.* **1994**, *116*, 3780. (b) Schultz, R. H.; Elkind, J. L.; Armentrout, P. B. *J. Am. Chem. Soc.* **1988**, *110*, 411.

(5) (a) Armentrout, P. B. *Annu. Rev. Phys. Chem.* **1990**, *41*, 313. (b) Eller, K.; Schwartz, H. *Chem. Rev.* **1991**, *91*, 1121.

(6) (a) Noll, R. J.; Yi, S. S.; Weisshaar, J. C. *J. Phys. Chem. A* **1998**, *102*, 386. (b) Yi, S. S.; Blomberg, M. R. A.; Siegbahn, P. E. M.; Weisshaar, J. C. *J. Phys. Chem. A* **1998**, *102*, 395.

(7) (a) Weisshaar, J. C. *Acc. Chem. Res.* **1993**, *26*, 213. (b) Weisshaar, J. C. *Adv. Chem. Phys.* **1992**, *82*, 213.

(8) (a) Holthausen, M. C.; Koch, W. *J. Am. Chem. Soc.* **1996**, *118*, 9932. (b) Holthausen, M. C.; Koch, W. *Helv. Chim. Acta* **1996**, *79*, 1939.

(9) Carroll, J. J.; Haug, K. L.; Weisshaar, J. C.; Blomberg, M. R. A.; Siegbahn, P. E. M.; Svensson, M. *J. Phys. Chem.* **1995**, *99*, 13955.

(10) (a) Siegbahn, P. E. M.; Blomberg, M. R. A. *J. Am. Chem. Soc.* **1992**, *114*, 10548. (b) Siegbahn, P. E. M.; Blomberg, M. R. A. In *Theoretical Aspects of Homogeneous Catalysis*; van Leeuwen, P. W. N. M., Morokuma, K., van Lenthe, J. H., Eds.; Kluwer: Dordrecht, Netherlands, 1995; pp 15−63.

(11) Stauffer, H. U.; Hinrichs, R. Z.; Schroden, J. J.; Davis, H. F. *J. Phys. Chem. A* **2000**, *104*, 1107.

(12) Hinrichs, R. Z.; Willis, P. A.; Stauffer, H. U.; Schroden, J. J.; Davis, H. F. *J. Chem. Phys.* **2000**, *112*, 4634.

(13) (a) Low, J. J.; Goddard, W. A., III *J. Am. Chem. Soc.* **1984**, *106*, 8321. (b) Low, J. J.; Goddard, W. A., III *Organometallics* **1986**, *5*, 609.

(14) Hinrichs, R. Z.; Schroden, J. J.; Davis, H. F. *J. Am. Chem. Soc.* **2003**, *125*, 861.

(15) Porembski, M.; Weisshaar, J. C. *J. Phys. Chem. A* **2001**, *105*, 6655.

(16) (a) Porembski, M.; Weisshaar, J. C. *J. Phys. Chem. A* **2001**, *105*, 4851. (b) Porembski, M.; Weisshaar, J. C. *J. Phys. Chem. A* **2000**, *104*, 1524.

(17) Bayse, C. A. *J. Phys. Chem. A* **2002**, *106*, 4226.

(18) Schroden, J. J.; Wang, C. C.; Davis, H. F. *J. Phys. Chem. A* **2003**, *107*, 9295.

(19) Willis, P. A.; Stauffer, H. U.; Hinrichs, R. Z.; Davis, H. F. *Rev. Sci. Instrum.* **1999**, *70*, 2606.

(20) Stauffer, H. U. Ph.D. Thesis, Cornell University, Ithaca, NY, 2000.

(21) Miller, W. B.; Safron, S. A.; Herschbach, D. R. *Discuss. Faraday Soc.* **1967**, *44*, 108.

(22) Levine, R. D.; Bernstein, R. B. *Molecular Reaction Dynamics and Chemical Reactivity*; Oxford University Press: Oxford, U.K., 1987; pp 247−260.

(23) Willis, P. A.; Stauffer, H. U.; Hinrichs, R. Z.; Davis, H. F. *J. Phys. Chem. A* **1999**, *103*, 3706.

(24) Stauffer, H. U.; Hinrichs, R. Z.; Willis, P. A.; Davis, H. F. *J. Chem. Phys.* **1999**, *111*, 4101.

(25) (a) Stauffer, H. U., Hinrichs, R. Z.; Schroden, J. J.; Davis, H. F. *J. Chem. Phys.* **1999**, *111*, 10758. (b) Schroden, J. J.; Teo, M.; Davis, H. F. *J. Chem. Phys.* **2002**, *117*, 9258. (c) Schroden, J. J.; Teo, M.; Davis, H. F. *J. Phys. Chem. A* **2002**, *106*, 11695.

(26) Center, R. E.; Mandl, A. *J. Chem. Phys.* **1972**, *57*, 4104.

(27) (a) Puddephatt, R. *Coord. Chem. Rev.* **1980**, *22*, 149. (b) Jennings, P. W.; Johnson, L. L. *Chem. Rev.* **1994**, *94*, 2241.

(28) (a) Periana, R. A.; Bergman, R. G. *J. Am. Chem. Soc.* **1986**, *108*, 7346. (b) Periana, R. A.; Bergman, R. G. *J. Am. Chem. Soc.* **1986**, *108*, 7332. (c) Periana, R. A.; Bergman, R. G. *J. Am. Chem. Soc.* **1984**, *106*, 7272.

(29) (a) Chen, Y.-M.; Armentrout, P. B. *J. Am. Chem. Soc.* **1995**, *117*, 9291. (b) Sunderlin L. S.; Armentrout, P. B. *J. Phys. Chem.* **1990**, *94*, 3589. (c) Fisher E. R.; Armentrout, P. B. *J. Phys. Chem.* **1990**, *94*, 1674. (d) Chen, Y.-M.; Sievers, M. R.; Armentrout, P. B. *Int. J. Mass Spectrom. Ion Processes* **1997**, *167*/*168*, 195.

(30) van Koppen, P. A. M.; Jacobson, D. B.; Illies, A.; Bowers, M. T.; Hanratty, A.; Beauchamp, J. L. *J. Am. Chem. Soc.* **1989**, *111*, 1991.

(31) (a) Chu, C. J.; Kafafi, Z. H.; Margrave, J. L.; Hauge, R. H.; Billups, W. E. *Organometallics* **2000**, *19*, 39. (b) Kline, E. S.; Hauge, R. H.; Kafafi, Z. H.; Margrave, J. L. *Organometallics* **1988**, *7*, 1512.

(32) (a) Dewar, M. J. S. *Bull. Soc. Chim. Fr.* **1951**, 79. (b) Chatt, J.; Duncanson, L. A. *J. Chem. Soc.* **1953**, 2939.

(33) Blomberg, M. R. A.; Siegbahn, P. E. M.; Svensson, M. *J. Phys. Chem.* **1992**, *96*, 9794.

(34) Siegbahn, P. E. M.; Blomberg, M. R. A.; Svensson, M. *J. Am. Chem. Soc.* **1993**, *115*, 1952.

(35) Crabtree, R. H. *The Organometallic Chemistry of the Transition Metals*; John Wiley & Sons: New York, 1994; p 291.
(36) (a) Grubbs, R. H.; Burk, P. L.; Carr, D. D. *J. Am. Chem. Soc.* **1975**, *97*, 3265. (b) Cundari, T. R.; Gordon, M. S. *Organometallics* **1992**, *11*, 55. (c) Rappe A. K.; Goddard, W. A. *J. Am. Chem. Soc.* **1982**, *104*, 448.
(37) Siegbahn, P. E. M. *Chem. Phys. Lett*. **1993**, *201*, 15.
(38) Spessard, G. O.; Miessler, G. L. *Organometallic Chemistry*; Prentice-Hall: Upper Saddle River, NJ, 1997; pp 118−119.
(39) Mingos, D. M. P. In *Comprehensive Organometallic Chemistry*; Wilkinson, G., Stone, F. G. A., Abel, E. A., Eds.; Pergamon Press: Oxford, U.K., 1982; Vol. 3, p 77.
(40) Hinrichs, R. Z. Ph.D. Thesis, Cornell University, Ithaca, NY, 2001.